Research Paper

Journal of Chemical Research

Journal of Chemical Research
November-December 1–10

DOI: 10.1177/17475198251387931
journals.sagepub.com/home/chl
Sage

A Comparative Evaluation of Antibacterial Activity of Metallic Nanoparticle Formulations Synthesized Using a Poly(amic) Acid

Maxwell Obumba[1], Naumih Noah[2] and Mildred Nawiri[1]

Abstract

Water is considered one of the most abundant natural resources, covering the largest proportion of the Earth's total surface. The availability of clean and safe water for domestic use, however, remains the most important scientific and technological challenge facing humanity presently. Disposal of human organic waste containing large volumes of deadly microbes, including *Streptococcus aureus* and *Escherichia coli*, has been cited as the major cause of water pollution and contamination. The increasing prevalence of these antibiotic-resistant pathogens in major water sources presents a critical challenge to public and environmental sustainability. Addressing this challenge calls for the development of novel, effective antimicrobial agents. This study reports the effect of synthesis temperature on the particle size and dispersion, which in turn influence the antimicrobial activity of silver (Ag), gold (Au), and bimetallic silver/gold (Ag/Au) nanoparticles synthesized and stabilized with a biodegradable poly(amic) acid PAA-polymer against *S. aureus* and *E. coli*. The synthesis of the different nanoparticle formulations was carried out in two different sets of temperatures: ambient (25 °C) and elevated temperatures (70 °C). The elevated temperature was kept at 70 °C to minimize imidization of PAA to polyimides, a process which occurs at temperatures above 100 °C. This ensured that the stability and structural integrity of PAA were preserved throughout the synthesis process. Nanoparticles synthesized at both ambient and elevated temperatures were characterized by cyclic voltammetry, ultraviolet–visible spectroscopy, and transmission electron microscopy. The results revealed spherical particles sized between 25 and 58 nm, with elevated temperatures yielding smaller, more uniformly dispersed nanoparticles. Elevated temperatures exhibited enhanced antibacterial activity against *E. coli* and *S. aureus* using disk diffusion assays. A higher antimicrobial activity exhibited by the bimetallic Ag/Au nanoparticles synthesized at elevated temperatures (Ag/Au NPs-HT) showed superior inhibition zone against *E. coli* (27.67 ± 1.53 mm) and *S. aureus* (23.67 ± 0.58 mm), outperforming their counterparts synthesized at ambient temperature ($p = 0.0088$; for *E. coli*) and all monometallic nanoparticles ($p < 0.0001$ for both *S. aureus* and *E. coli*). Statistically, Ag/Au NPs-HT exhibited a stronger antimicrobial activity as compared to Vancomycin, a commercial clinical antibiotic against both *S. aureus* ($p < 0.0007$) and *E. coli* ($p < 0.0007$). These findings highlight a synergistic effect when combining silver and gold and underscore synthesis temperatures as a crucial factor in optimizing the antimicrobial performance of Nobel metal nanoparticles, with potential application in environmentally sustainable and cost-effective water purification systems.

Keywords

antimicrobial activity, *Escherichia coli*, nanoparticles synthesis, nanotechnology, poly(amic) acid, *Streptococcus aureus*, waste water

Received: 20 July 2025; accepted: 26 September 2025

Graphical abstract

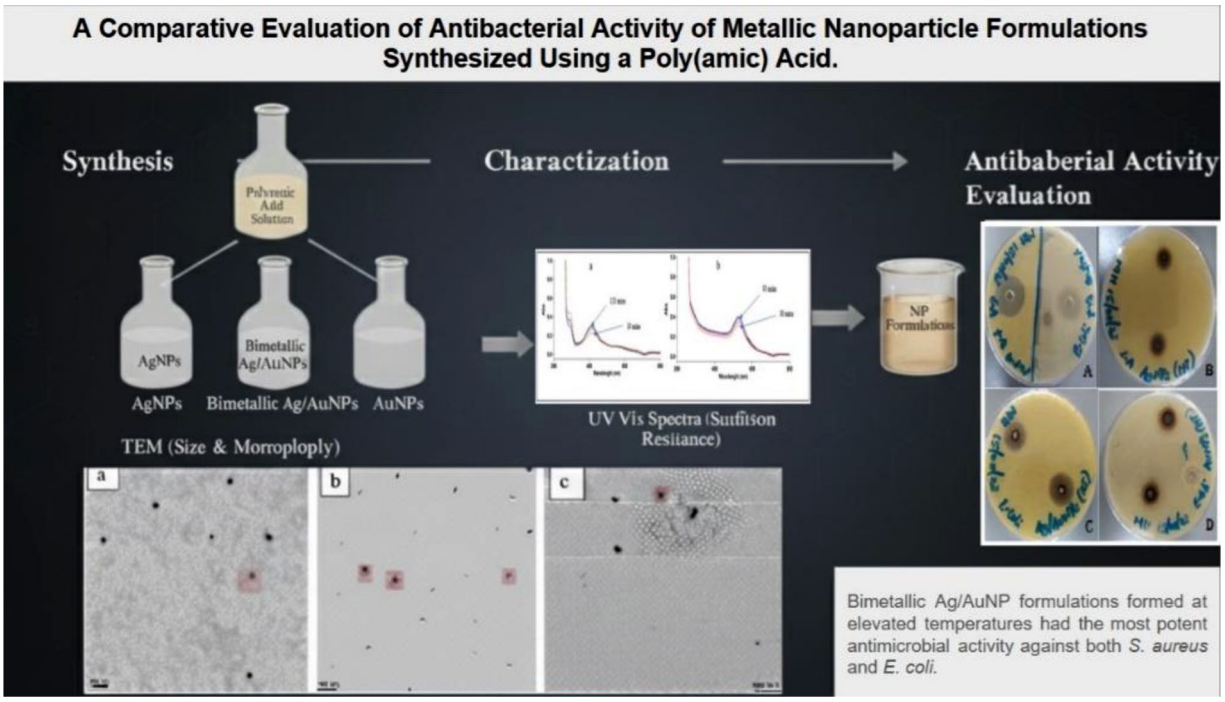

Introduction

Water is one of the most essential resources on the planet-earth without which there cannot be life. It is important in many processes, biological and chemical, in the human body. However, the availability of clean and safe water for drinking remains a critical global challenge, aggravated by escalating pollution levels, rapid global population growth, and climate change. In Kenya, water pollution is largely as a result of the discharge of partially treated or untreated human organic wastes from urban centers into surface water bodies, leading to microbial contamination by harmful pathogens such as *Escherichia coli* (*E. coli*) and *Streptococcus aureus* (*S. aureus*), which have been linked to the prevalence of waterborne diseases, including diarrhea, dysentery, and jaundice.[1] According to the World Health Organization,[2] Kenya reported over 37,655 deaths attributed to water-related illnesses in 2018 alone, representing nearly 14.75% of total mortality. This statistic emphasizes the urgency of achieving Sustainable Development Goal 6 (SDG 6): ensuring availability and sustainable clean and safe water for all.

Recent advances in nanotechnology offer promising approaches to water purification and remediation, particularly through the application of noble metallic nanoparticles (NPs). Silver nanoparticles (AgNPs) and gold nanoparticles (AuNPs) are of particular interest due to their high surface-to-volume ratio and unique physicochemical, catalytic, and optical properties, which contribute to their application as ideal candidates for antimicrobial agents. Research has clearly shown that the antimicrobial activity of these nanoparticles is influenced by physicochemical properties such as shape, particle size, and dispersion.[3] These properties are, in turn, significantly influenced by the methodology and conditions adopted for synthesis, most notably, the temperature at which the nanoparticles are synthesized.[4]

Nanoparticles synthesized at elevated temperatures tend to possess higher surface energy, better size distribution, and greater crystallinity, which overly enhances their antimicrobial activity.[5] On the other hand, synthesis at ambient temperatures offers environmental and economic benefits but often results in particles with broader size distributions and lower crystallinity, which may generally compromise antimicrobial efficiency. Although AgNPs and AuNPs are well known for their antimicrobial activity, the influence of synthesis conditions, particularly temperature, on their functional and structural efficacy remains inadequately investigated, creating a critical knowledge gap on how to optimize the synthesis of metallic nanoparticles for enhanced antimicrobial performance against lethal waterborne bacteria such as *E. coli* and *S. aureus*. Presently, studies predominantly focus on monometallic nanoparticles synthesized under ambient temperatures, with limited comparison to bimetallic synthesis at different temperatures.

Furthermore, a significant challenge in nanoparticle synthesis is stabilization of the nanoparticles to prevent agglomeration, as agglomeration commonly caused by particles'

[1]Chemistry Department, Kenyatta University, Nairobi, Kenya
[2]School of Pharmacy and Health Sciences, United States International University-Africa, Nairobi, Kenya

Corresponding author:
Naumih Noah, School of Pharmacy and Health Sciences, United States International University-Africa, P.O. Box 14634-00800, Nairobi, Kenya.
Email: mnoah@usiu.ac.ke

high surface energy has been reported to reduce antimicrobial performance.[6] Stabilizers or capping agents are often used to prevent particle growth and aggregation. However, an ideal stabilizer must not mask the functional properties of the nanoparticles.[7] While polyaniline has been explored as both a reducing agent and stabilizer in AgNPs and AuNPs synthesis, its practical application has been compromised due to its poor solubility in a range of solvents, low processability, and its nonbiodegradable nature. In this context, Poly(amic) acid (PAA) offers a promising alternative, although its potential as both reductant and stabilizer has not been sufficiently explored. PAAs are soluble in a wide range of dipolar aprotic solvents, are biodegradable, have excellent mechanical stability, and possess high cation-complexing ability, making them appropriate for application as both reductants and stabilizers in nanoparticle synthesis.[7] In this study, we report the application of synthesized nanostructured poly(amic) acid (PAA) in the synthesis of AgNPs, AuNPs, and bimetallic Ag/AuNPs under both ambient and elevated temperatures, evaluating their structural properties and antimicrobial efficacy against *E. coli* and *S. aureus*. By investigating the influence of synthesis temperature on the antimicrobial performance of AgNPs and AuNPs, this study aims to address a crucial gap in the application of noble nanoparticles for the treatment of common microbes found in wastewater.

Materials and methods

Reagents

4,4′-Oxydianiline (ODA, 97%), 3,3,4,4-Benzophenonetetracarboxylic dianhydride (BTDA, 98%), Dimethylformamide (DMF), *N*-Methyl-2-pyrrolidone (NMP, anhydrous, 99.5%), HPLC water, Silver nitrate ($AgNO_3$), gold III chloride ($AuCl_3$), *Escherichia coli* cells (ATCC 25922, Gram-negative), *Streptococcus aureus* cells (ATCC 6538), Vancomycin (MIC=2 $\mu g\,mL^{-1}$), Sodium phosphate monobasic (NaH_2PO_4), Sodium phosphate dibasic (Na_2HPO_4), and Broth were purchased from Sigma Aldrich, USA. Silver nitrate ($AgNO_3$) and gold III chloride ($AuCl_3$) where Glassware was treated with aqua regia solution (1V HNO_3: 3V HCl) and rinsed thoroughly with distilled water.

Synthesis of poly(amic) acid-PAA

PAA was synthesized via a modified polycondensation method as described by Cao et al.[8] Briefly, 210.25 mg of ODA was dissolved in 4 mL NMP under nitrogen and stirred at ambient (25 °C) until complete dissolution of ODA was obtained. Subsequently, 322.00 mg of BTDA was added gradually while maintaining a nitrogen purge. The reaction mixture was stirred at 500 rpm for 24 h while protected from light using aluminum foil. The formation of a yellow viscous solution indicated successful synthesis of PAA. The synthesized PAA was stored in the freezer for later use in the synthesis of nanoparticles.

Synthesis and stabilization of silver nanoparticles- AgNPs

Silver nanoparticles were synthesized at two different temperatures: ambient (25 °C) and elevated (70 °C) in a thermostatically controlled oil bath. The synthesis was done by chemical reduction using PAA as both reductant and stabilizer, following a modified method as described by Kimotho and coworkers.[9] 5.00 mg of $AgNO_3$ was dissolved in 3.00 mL of NMP, then 28 µL of PAA was added. The mixture was stirred at 500 rpm under nitrogen for 25 h in the dark. Reactions were conducted under two different temperature conditions:

- AgNPs-HT: elevated temperatures 70 °C)
- AgNPs-RT: ambient Temperature (25 °C)

Silver ions (Ag^+) reduction was monitored using UV-vis spectroscopy (Hewlett Packard 8453; 300–700 nm range, 1 cm quartz cuvette) at intervals. A PAA-NMP solution was used as a control.

Synthesis and stabilization of gold nanoparticles-AuNPs

Synthesis of AuNPs was modified from the method previously reported by Kimotho and coworkers,[9] as well as Nguyen and coworkers.[10] Specifically, 6.29 mg of $AuCl_3$ was dissolved in 3.00 mL NMP, followed by the addition of 28 µL of PAA. The mixture was stirred at 500 rpm and incubated for 25 h in the dark. Reactions were conducted under two different temperature conditions:

- AuNPs-RT: ambient Temperature (25 °C)
- AuNPs-HT: elevated temperatures 70 °C)

Gold ions (Ag^+) reduction was conducted as described in Section 2.3. A PAA-NMP solution was used as a control.

Synthesis of silver and gold bimetallic nanoparticles-Ag/AuNPs

Bimetallic Ag/Au NPs were synthesized by sequential reduction. First, 5.00 mg of $AgNO_3$ was dissolved in 3.00 mL of NMP, followed by the addition of 28 µL PAA. The mixture was stirred for 1 h under nitrogen at either ambient (25 °C) or elevated temperature (70 °C). Upon cooling, 6.29 mg of $AuCl_3$ was added, and the mixture was stirred under nitrogen for 24 h. The resulting mixtures were labeled as Ag/AuNPs-RT and Ag/AuNPs-HT, based on the temperature used during the initial silver reduction step. Each setup was covered in aluminum foil to keep off light.

Antibacterial activity

The antimicrobial performance of synthesized AgNPs, AuNPs, and Ag/Au Bimetallic NPs was assessed against *Escherichia coli* cells (Gram-negative) and *Streptococcus aureus* (Gram-positive), using the agar well diffusion method, following the guidelines by Clinical and Laboratory Standards Institute.[11] Each bacterial strain was independently cultured in nutrient broth and incubated at 37 °C for a duration of 24 h. Thereafter, cultures were uniformly spread onto Mannitol salt agar and MacConkey agar using a sterile swab. Subsequently, 8 mm diameter wells were

punched into the agar, and loaded with 100 μL of the synthesized nanoparticles (AgNPs, AuNPs, or Ag/AuNPs, at 1.0 mg mL)$^{-1}$. The plates were then incubated at 37 °C for 24 h in an upright position. Controls were:

- Negative control: PAA solution in NMP.
- Positive Control: Vancomycin (30 μL mL)$^{-1}$

Zones of inhibition were measured in millimeters using a digital vernier caliper. Each assay was conducted in triplicate.

Characterization techniques

Characterization of the synthesized nanoparticles (AgNPs, AuNPs, and bimetallic Ag/AuNPs) was done using spectroscopic, electrochemical, and microscopic techniques to assess the physicochemical properties and functionality, particularly those influenced by synthesis temperature.

UV-visible spectra analysis. The UV-vis absorption spectrum of the nanoparticles synthesized at different temperatures was monitored using a UV-vis spectrometer (Hewlett-Packard 8453; 300–800 nm range, 1 cm quartz cuvette) operating in dual-beam mode at room temperature. The spectral measurements were recorded at intervals during the 25 h of incubation to track the progression of nanoparticle formation and the distribution of nanoparticles. SPR bands arise from the interaction between the conduction electrons on the nanoparticle surface and the incident electromagnetic radiation, and it is sensitive to the size of particles, shape, and degree of aggregation.[12] Particle size estimates were further derived using Mie's theoretical equation,[13] which relates the quantum confinement-induced bandgap shift to particle size:

$$E_{nanoparticle} - E_{bulk} = \frac{h^2\pi^2}{2\mu R^2} + \frac{1.8e^2}{\varepsilon R}$$

where $E_{nanoparticle}$ and E_{bulk} are the band gaps (eV) of the sample and the bulk semiconductors respectively, μ is the electron–hole reduced effective mass, h is the Planck's constant (6.62607 × 10^{-}34 m^2 kg s)$^{-1}$, ε is the dielectric constant, R is the radius of the nanoparticle confinement region, and e is the elementary electric charge (1.6022 × 10^{-19} C).[14]

Cyclic Voltammetry (CV) method. Cyclic Voltammetry was employed to study the electrochemical characteristics and confirm the identity of the synthesized nanoparticles. The protocol was modified from the work reported by Ndikau and coworkers.[15] Synthesized nanoparticles were independently immobilized onto a glassy carbon electrode (the working electrode) by drop-casting and air-dried for about 10 min. Ag/AgCl (3 mol L^{-1} KCl) was used as the reference electrode, 0.05M Phosphate Buffer Solution (PBS) at pH 7.4, was used as the electrolyte, and platinum wire as the counter electrode. Scans were performed in the potential range of −1000 mV to +1000 mV with a switching potential of 800 mV. The scan rate was varied between 20 and 100 mV s^{-1}.

Transmission electron microscopy (TEM). TEM was used to determine the particle shape and size, and morphological characteristics of the synthesized nanoparticles. Imaging was done using a JEOL 2100F Transmission Electron Microscope operating at an acceleration voltage of 200 kV. Samples were prepared by mounting a few drops of the synthesized nanoparticles onto the carbon-coated copper grid, followed by drying under a dryer for 5 min.[16] The particle sizes were estimated using ImageJ software.

Statistical analysis. All experiments were performed in triplicate, and measurements were expressed as mean ± standard deviation (SD). Statistically significant differences in antibacterial activity (Measured by zone of inhibition) between nanoparticles synthesized at ambient (25 °C) and elevated temperatures (70 °C), and among different nanoparticle formulations, were assessed using one-way Analysis of Variance (ANOVA). Results were considered statistically significant at $p < 0.05$. Tukey's Honest Significant Difference (HSD) post hoc test was employed to determine significant variations between groups. The correlation between synthesis temperature, nanoparticle size, and antimicrobial efficacy was assessed using Pearson correlation coefficients. We recommend that to validate the statistical significance of correlations between antimicrobial efficacy and particle size, further investigations should include power analysis to formally establish the required sample size. All analyses were conducted using GraphPad Prism 9.0.

Environmental and ethical considerations. Careful attention to considerations was taken into account with the aim of developing eco-friendly nanoparticles for antimicrobial activity. All the protocols employed were in accordance with acceptable safety and environmental management guidelines. There were no human or animal subjects in this study. The bacterial strains used were standard laboratory strains permitted for use under the Biosafety Level 2 (BSL 2) protocols.

Results and discussion

This study aimed to evaluate how synthesis temperature influenced AgNPs, AuNPs, and bimetallic Ag/AuNPs properties, such as Size, morphology, and dispersion, and how these physicochemical properties affect antimicrobial efficacy against *Escherichia coli* cells (ATCC 25922, Gram-negative) *Streptococcus aureus* cells (ATCC, 6538, Gram-positive). NPs synthesized at ambient and elevated temperatures were characterized using UV-vis spectroscopy, CV, and TEM. The Antimicrobial activities were assessed using the agar well diffusion assay. The findings in this study were discussed with reference to existing current literature and in relation to the proposed role of PAA as both a reductant and a stabilizer.

Cyclic voltammetry (CV) employed, revealed distinct anodic peaks for AgNPs and AuNPs, with AuNPs showing

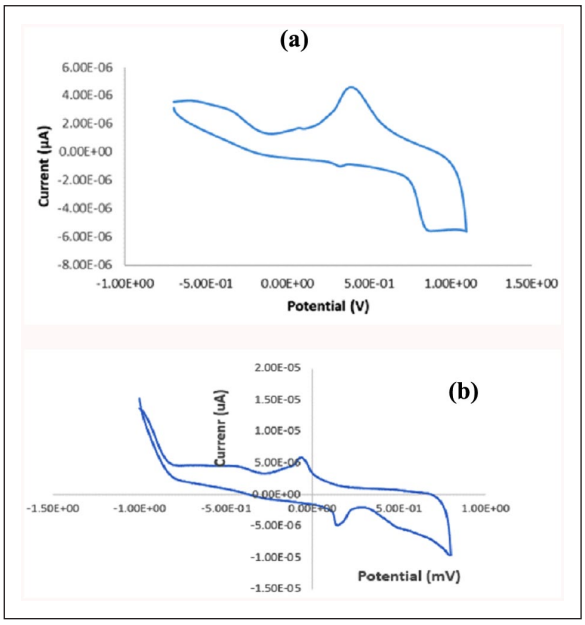

Figure 1. Cyclic voltammogram of synthesized AgNPs at 20 mV scan rate (a) and AuNPs at 20 mV scan rate (b).

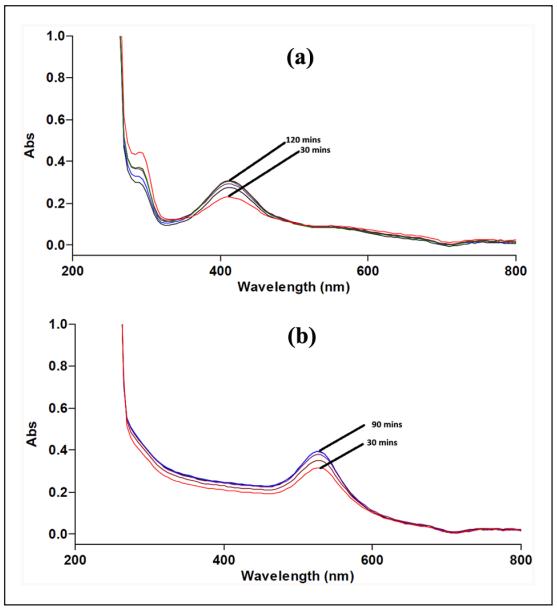

Figure 2. UV-vis spectra of AgNPs (a) and AuNPs (b) showing a change in absorbance with an increase in reaction time.

an oxidation peak at -530 mV and AgNPs at +407 mV as illustrated in Figure 1(a) and (b), These results correspond closely with previously reported values,[17] which validates the identity of the synthesized AgNPs and AuNPs. The comparison of cyclic voltammograms of known standards with those of the synthesized NPs further validated the presence of Ag and Au in their nanoparticulate form. These results confirmed the successful reduction of silver and gold ions by PAA into their respective nanoparticles. It was also clear that the scan rate had negligible effect on the peak position, suggesting stable redox behavior of the synthesized nanoparticles, a desirable property in the applications of nanoparticles that require chemical integrity and resistance to rapid degradation under testing conditions. It was also clear that the scan rate had a negligible effect on the peak position, suggesting stable redox behavior of the synthesized nanoparticles, a desirable property in the applications of nanoparticles that require chemical integrity and resistance to rapid degradation under testing conditions. This clearly suggests the chemical stability of the synthesized NPs under electrochemical procedures.[18]

The UV-vis spectra revealed characteristic SPR peaks for both silver and gold nanoparticles. The AgNPs exhibited characteristic SPR peaks in the region of 423–438 nm, while AuNPs displayed broader SPR peaks in the region of 518 to 548 nm. These results confirm the successful synthesis of AgNPs and AuNPs and are consistent with the optical behavior of the respective nanoparticles.[19,20] Using Mie's theory, the estimated size for AuNPs range from 24 to 30 nm, and for AgNPs from 26 to 32 nm. Notably, AgNPs were generally larger than the AuNPs, suggesting that PAA acts more effectively as a stabilizer for the AuNPs.[14] Stabilization of NPs could also be attributed to their excellent mechanical stability, high cation-complexing ability with the NP that helps in the prevention of aggregation.[21] In Figure 2, the absorbance values of the nanoparticles revealed a steady increase with reaction time until reaching a plateau, indicating completion of the reduction process and a stable state of the NPs during the monitoring period. For the synthesis of AgNPs at ambient temperature (AgNPs-RT), this plateau was reached at 120 min, while for AgNPs synthesized at elevated temperature (AgNPs-HT), the reaction completion occurred at 90 min. This result proves that nucleation and particle growth occur at a faster rate with elevated temperatures. In addition, a narrower, blue shift in SPR peaks was observed in NPs synthesized at elevated temperatures, moving from longer wavelengths to shorter wavelengths. For Example, AuNPs nanoparticles synthesized at ambient temperatures were detected around 548 nm, which was higher than the peaks for the AuNPs synthesized at elevated temperatures, which were detected at about 518 nm. This shift indicated a reduction in particle size, consistent with the known correlation between SPR peak position and particle size as described by Mie's theory. These findings show that lower temperatures favor the aggregation of particles. This finding was supported by the TEM results.

The TEM images revealed that both AgNPs and AuNPs synthesized under elevated and ambient temperatures were predominantly spherical. Differences in size distribution varied based on synthesis temperatures:

- AgNPs-HT ranged from 26 to 32 nm in diameter, while AgNPs-RT measured between 34 and 58 nm.
- AuNPs-HT ranged from 19 to 28 nm in diameter, while AgNPs-RT measured between 27 and 43 nm. These results align with the size estimates obtained through UV–vis spectroscopy and Mie theory calculations.

A key observation was that nanoparticles synthesized at ambient temperatures showed more visible agglomeration compared to those synthesized at elevated temperatures, further emphasizing that lower reaction temperatures facilitate particle growth and aggregation. This aggregation

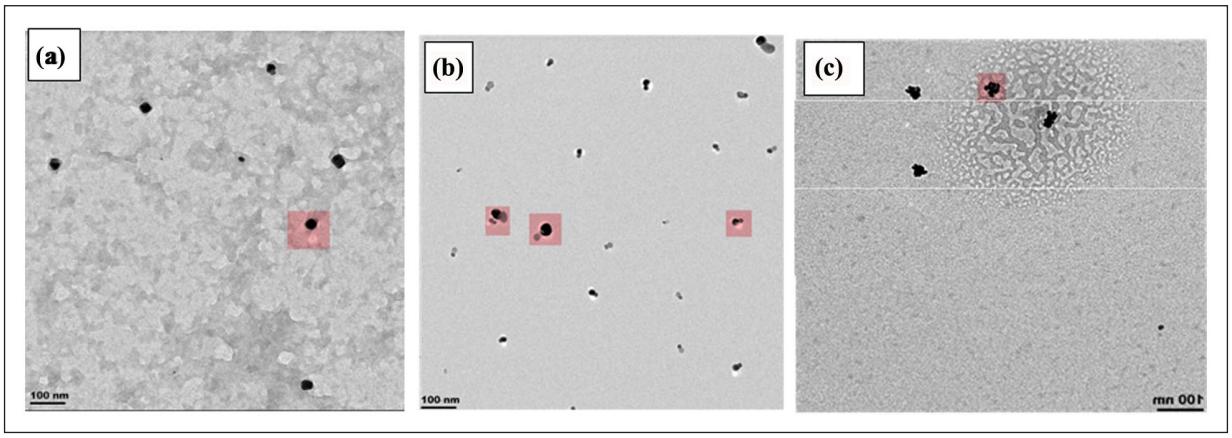

Figure 3. TEM images of (a) AgNPs at 70 °C, (b) AgNPs at 25 °C, and (c) AuNPs at 25 °C.

Table 1. Mean standard deviation of Zone of inhibition (mm) for the AgNPs, AuNPs, Ag/Au Bimetallic nanoparticle formulations and the controls against *S. aureus* and *E. coli.*

Nanoparticle formulation/ Controls	Zone of inhibition (mm)	
	S. aureus	*E. coli*
AuNPs (RT)	18.33 ± 0.58	17.33 ± 0.58
AuNPs (HT)	19.67 ± 0.58	19.33 ± 0.58
AgNPs (RT)	16.00 ± 0.00	16.33 ± 0.58
AgNPs (HT)	16.00 ±1.00	18.00 ± 1.00
Ag/AuNPs (RT)	22.33 ± 0.58	24.33 ± 0.58
Ag/AuNPs (HT)	23.67 ± 0.58	27.67 ± 0.53
Vancomycin (+ve control)	26.33 ± 0.58	23.33 ±1.53
Negative control	0.00 ± 0.00	0.00 ± 0.00

could be due to the slower nucleation and less effective stabilization by PAA during synthesis at ambient temperatures. In contrast, synthesis at elevated temperatures promoted the formation of smaller, well-dispersed nanoparticles, which is advantageous for antimicrobial performance. The images (Figure 3) also revealed that, despite some aggregation, the nanoparticles were not in direct contact, suggesting the effective role of PAA in capping and stabilization, which minimized particle-particle fusion (particle growth) even under less controlled conditions, as noted by Javed et al.[22] Our earlier findings established that PAA can stabilize monodispersed AgNPs and AuNPs for periods exceeding 90 days under ambient conditions, highlighting its capacity to maintain nanoparticle stability during and after synthesis while ensuring reproducibility—a vital property in real-life applications.[14]

These morphological properties directly correlate with the antimicrobial findings of the study: stronger antimicrobial activity was demonstrated by smaller, more monodispersed nanoparticles synthesized at elevated temperatures as opposed to those synthesized at ambient temperature. Smaller particles have a larger surface area, which enhances interaction with bacterial membranes and promotes greater oxidative stress, ultimately improving their antimicrobial effectiveness.

The antibacterial activity assays against *S. aureus* and *E. coli* were performed in triplicate, and the corresponding inhibition zone diameters were reported as mean ± standard deviation (SD) (Table 1), and visualized in Figure 4. The statistical tests included: statistical significance, assessed using one-way ANOVA, Tukey's Honest Significant Difference (HSD) post hoc test, and Pearson correlation analysis (Table 2–4). The analysis aimed to evaluate the effect of synthesis temperature and nanoparticle type on antimicrobial performance against *S. aureus* and *E. coli.*

One-way Anova demonstrated that all nanoparticle types exhibited significant differences in their antimicrobial activity compared to the negative control against both *S. aureus* and *E. coli* ($p < 0.0001$). This confirms a measurable inhibiting property on both *S. aureus* and *E. coli* by all the nanoparticle types. Bimetallic Ag/AuNPs-HT demonstrated the largest inhibition zone, with a zone diameter of 23.67 ± 0.58 mm for *S. aureus* and 27.67 ± 1.53 mm for *E. coli*, significantly exceeding their monometallic (AgNPs and AuNPs) counterparts ($p < 0.0001$ for both *S. aureus* and *E. coli*; Table 2) and Vancomycin ($p = 0.0007$ for *S. aureus* and *E. coli*), pointing evidence to synergistic antimicrobial effect of combining Au and Ag, which enhances their activity beyond that of monometallic nanoparticles. This finding is consistent with previous studies, demonstrating ROS generation of ROS and combined action in membrane distortion by bimetallic nanoparticles attributed to the combination effect of improved particle stability, surface energy, redox properties, and controlled ion release in the medium.[23–26] In addition, Ag/AuNPs synthesized at ambient temperatures were effective but statistically equivalent to Vancomycin activity ($p = 0.8826$ for *E. coli*).

Surprisingly, AuNPs showed stronger antimicrobial activity as compared to their silver counterparts in most cases, particularly at elevated temperature, which contradicts the previously reported trends where the antimicrobial performance of AgNPs is superior.[27] This inconsistency may be due to:

- Variations in particle size as depicted by TEM indicate that smaller, well-dispersed AuNPs have a larger effective surface area, which enhances interaction with microbe membranes and promotes enhanced oxidative stress, leading to greater Reactive Oxygen Species (ROS) generation. This greater ROS generation is a

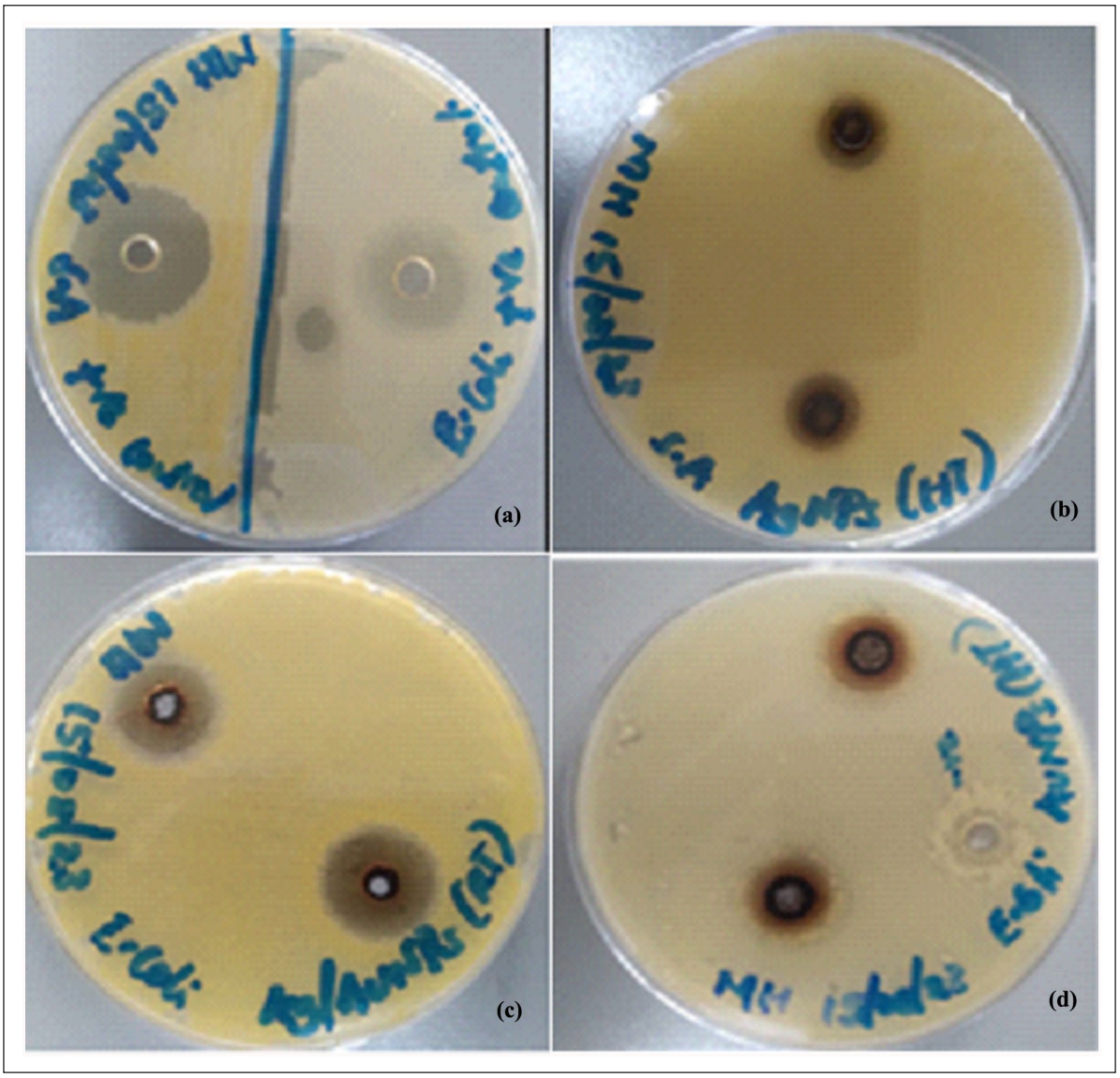

Figure 4. Visible zones produced by +ve control against *E. coli* (a), AgNPs (HT) against *S. aureus* (b), Ag/Au Bimetallic NPs (RT) against *E coli* (c), AuNPs (HT) against *E. coli* (d).

Table 2. Tukey's HSD Pairwise Statistical comparisons of antimicrobial activity: Elevated temperature versus ambient temperature synthesized Ag, Au, and bimetallic Ag/Au nanoparticles and Vancomycin against *S. aureus* and *E. coli*.

	Significance (p-value)	
Comparison	*S. aureus*	*E. coli*
Ag/AuNPs-HT vs Vancomycin (+ve control)	0.0007 (superior)	0.0007 (superior)
Ag/AuNPs-HT vs Negative control	<0.0001	<0.0001
Ag/AuNPs-HT vs Ag/AuNPs-RT	0.1552	0.0088
Ag/AuNPs-HT vs AuNPs-HT	<0.0001	<0.0001
Ag/AuNPs-RT vs AuNPs-HT	0.0007	0.0001
Ag/AuNPs-RT vs AuNPs-RT	<0.0001	<0.0001
AuNPs-HT vs AuNPs-RT	0.1552	0.2185
AgNPs-HT vs AgNPs-RT	>0.9999	0.4096
AuNPs-HT vs AgNPs-HT	<0.0001	0.6608
AuNPs-RT vs AgNPs-HT	0.0028	0.9846
AuNPs-RT vs AgNPs-RT	0.0028	0.8826

critical mechanism in facilitating the interruption of bacterial metabolic functions and membrane degradation. It is also possible that AuNPs might have been better stabilized by PAA, potentially possessing a more homogeneous surface charge distribution, resulting in minimal agglomeration. Agglomeration reduces the effective surface area, shielding active sites necessary for antimicrobial activity.[28]

Table 3. Pearson correlation between nanoparticle size (nm) and zone of inhibition (mm) for both *S. aureus* and *E. coli*.

Metric	*S. aureus*	*E. coli*
Pearson (r)	–0.7191	–0.6954
95% Confidence Interval	–9.666 to 0.2220	–0.9633 to 0.2667
R^2 (Coefficient of Determination)	0.5171 (51.7%)	0.4835 (48.4%)
P-Value (two-tailed)	0.1073	0.1251

Table 4. Pearson correlation between nanoparticle size (nm) and synthesis temperature.

Metric	Value
Pearson (*r*)	–0.5342
95% Confidence Interval	–0.9388 to 0.4897
R^2 (Coefficient of Determination)	0.2853
p-value (two-tailed)	0.2750

- Presence of residual ionic species (Au^+ and Au^{3+} ions, that may have remained unreduced) in the mixture achieved after reduction may have caused additional cytotoxicity beyond those of the NPs. The residual ions interact with microbes by binding with biomolecules or disrupting essential cellular functions.[29,30]
- Gram-negative bacteria may be more susceptible to oxidative stress induced by smaller nanoparticles.

Pearson correlation revealed a strong negative relationship between particle size and antimicrobial activity for both *E. coli.* ($r = -0.6954$) and *S. aureus* ($r = -0.7191$), reaffirming that smaller nanoparticles tend to exhibit stronger antimicrobial activity (Table 3), agreeing with Franci and coworkers.[31] However, the relationship was not statistically significant at the $p = 0.05$ level ($p = 0.1073$), which could be due to potential factors such as existence of a threshold (plateau effect) below which further reductions on nanoparticle size might not significantly enhance activity, monomer concentration or nanoparticle properties like shape, size distribution, surface distribution which come into play to determine biological and optical properties of nanoparticles.[32,33] Further, a moderate negative relationship ($r = -0.5342$) between particle size and synthesis temperature, indicating that elevated synthesis temperatures generally yield particles with smaller sizes, although there was no noticeable statistical significance in the trend ($p = 0.2750$; Table 4).

Conclusion

In this study, AgNPs, AuNPs, and bimetallic Ag/AuNPs were successfully synthesized using PAA as a dual-function reductant and capping agent, resulting in predominantly spherical and stabilized nanoparticles. The results demonstrated the critical interplay between nanoparticle composition, particle size, and synthesis temperature in determining antimicrobial activity. Synthesis at elevated temperature consistently produced smaller, less aggregated, and more monodispersed nanoparticles with enhanced antimicrobial properties. Although the study reports the PAA efficacy in providing stabilization of nanoparticles during synthesis, its long-term efficacy under different storage conditions needs to be investigated. Elevated temperatures accelerate nucleation, increasing the solubility of stabilizers, enhancing their efficiency in preventing agglomeration, resulting in smaller and more monodispersed particles. Bimetallic Ag/AuNP formulations, especially those synthesized at elevated temperatures, exhibited the most potent antimicrobial performance against both *S. aureus* and *E. coli*, outperforming not only their monoatomic counterparts but also Vancomycin, which was used as a standard clinical antibiotic. This enhanced activity is attributed to the synergistic effect of Ag and Au, which arise from a combination of factors including improved generation of reactive ionic species and redox recycling combined with the influence of reduced nanoparticle size, collectively facilitating extra efficiency in microbial membrane degradation, interruption in the normal metabolic function of bacteria, and oxidative stress induction. These findings suggest that synthesis of nanoparticles for antimicrobial applications should not only prioritize size and stability of nanoparticles but also consider bimetallic compositions synthesized at controlled conditions to maximize synergic effects. The demonstrated strong antimicrobial activity of the investigated Bimetallic NPs, particularly those synthesized at elevated temperatures, positions them as promising candidates for real-life application in wastewater purification systems and may be considered alternatives in combating the rise in multidrug-resistant strains of bacteria. To enhance scalable synthesis, nanoparticles can be usefully integrated into coating or tangential flow filtration media, to effectively eliminate microbes, thereby enhancing public health status. However, practical implementation faces critical challenges, including the cost of production, public acceptance, sustainability, environmental and biological safety issues, highlighting the need for further focused investigations to address these barriers before large-scale implementation can be realized. Further research is recommended to understand the mechanisms underlying synergic effects, clinical safety, and recycling techniques of these nanoparticle formulations for their potential application in wastewater treatment. One possibility may involve evaluating magnetic nanoparticles, which can be easily isolated using a magnetic field.

Acknowledgments

We thank the Organization for Women in Science for the Developing World (OWSD) for financing this project, USIU-Africa for the laboratory space and instrumentation, Kenyatta University, and the Teachers Service Commission.

ORCID iD

Naumih Noah https://orcid.org/0000-0002-2285-4475

Ethical considerations

This paper does not contain any studies with human or animal participants.

Consent to participate

This paper has no human participants, and informed consent is not required.

Consent for publication

Not applicable.

Funding

The authors disclosed receipt of the following financial support for the research, authorship, and/or publication of this article: This work was funded by the Organization for Women in Science for the Developing World (OWSD) under the award agreement 4500429478.

Declaration of conflicting interests

The authors declared no potential conflicts of interest with respect to the research, authorship, and/or publication of this article.

Data availability statement

Data is available from the corresponding author upon request.

References

1. Bashir I, Lone FA, Bhat RA, et al. Concerns and threats of contamination on aquatic ecosystems. In: Hakeem KR, Bhat RA and Qadri H (eds) *Bioremediation and biotechnology: sustainable approaches to pollution degradation*. Cham: Springer, 2020, pp. 1–26.
2. World Health Organization. *Drinking water: key facts*. Geneva, Switzerland: World Health Organization, 2023. https://www.who.int/news-room/fact-sheets/detail/drinking-water (accessed 9 October 2025).
3. Rónavári A, Igaz N, Adamecz DI, et al. Green silver and gold nanoparticles: biological synthesis approaches and potentials for biomedical applications. *Molecules* 2021; 26(4):844.
4. Lee SH and Jun BH. Silver nanoparticles: synthesis and application for nanomedicine. *Int J Mol Sci* 2019; 20(4): 865.
5. Mobarak MB, Sikder MDF, Muntaha KS, et al. Plant extract-mediated green-synthesized CuO nanoparticles for environmental and microbial remediation: a review covering basic understandings to mechanistic study. *Nanoscale Adv* 2025; 7: 2418–2445.
6. Kulkarni N and Muddapur U. Biosynthesis of metal nanoparticles: a review. *J Nanotechnol* 2014; 2014: 510246.
7. Kariuki VM, Yazgan I, Akgul A, et al. Synthesis and catalytic, antimicrobial and cytotoxicity evaluation of gold and silver nanoparticles using biodegradable, π-conjugated polyamic acid. *Environ Sci Nano* 2015; 2: 518–527.
8. Cao C, Liu L, Ma X, et al. Synthesis and properties of fluorinated copolymerized polyimide films. *Polímeros* 2020; 30: e2020017.
9. Kimotho I, Noah NM, Nawiri M, et al. Fabrication of nanostructured polyamic acid membranes for antimicrobially enhanced water purification. *Adv Polym Technol* 2020; 2020: 7362789.
10. Nguyen QK, Hoang TH, Bui XT, et al. Synthesis and application of polycation-stabilized gold nanoparticles as a highly sensitive sensor for molecular cysteine determination. *Microchem J* 2021; 168: 106481.
11. Clinical and Laboratory Standards Institute. *Performance Standards for Antimicrobial Susceptibility Testing; Twenty-Second Informational Supplement*. CLSI Document M 100-S22. Wayne, PA: Clinical and Laboratory Standards Institute, 2012. https://www.scirp.org/reference/referencespapers?referenceid=1617174 (accessed 9 October 2025).
12. Krajczewski J, Kołątaj K and Kudelski A. Plasmonic nanoparticles in chemical analysis. *RSC Adv* 2017; 7: 17559–17576.
13. Mie G. Beiträge zur Optik trüber Medien, speziell kolloidaler Metallösungen. *Ann Phys* 1908; 330: 377–445.
14. Obumba M, Noah N and Nawiri M. Room temperature synthesis and stabilization of silver and gold nanoparticles using polyamic acid. *J Kenya Chem Soc* 2023; 16: 20–24.
15. Ndikau M, Noah NM, Andala DM, et al. Green synthesis and characterization of silver nanoparticles using Citrullus lanatus fruit rind extract. *Int J Anal Chem* 2017; 2017: 8108504.
16. Wen H, Luna-Romera JM, Riquelme JC, et al. Statistically representative metrology of nanoparticles via unsupervised machine learning of TEM images. *Nanomaterials* 2021; 11(10): 2620.
17. El-Aswer E, Gaber S, Zahran M, et al. Characterization of biosynthesized silver nanoparticles by Haplophyllum tuberculatum plant extract under microwave irradiation and detecting their antibacterial activity against some wastewater microbes. *Desalination Water Treat* 2020; 195: 275–285.
18. Espinoza R, Cahua DV, Magro K, et al. A contactless method for measuring the redox potentials of metal nanoparticles. *J Phys Chem Lett* 2024; 15: 12243–12247.
19. Ngumbi P, Mugo S and Ngaruiya J. Determination of gold nanoparticles sizes via surface plasmon resonance. *IOSR J Appl Chem* 2018; 11: 25–29.
20. Wan Mat Khalir WKA, Shameli K, Jazayeri SD, et al. Biosynthesized silver nanoparticles by aqueous stem extract of Entada spiralis and screening of their biomedical activity. *Front Chem* 2020; 8: 620.
21. Okello VA, Du N, Deng B, et al. Environmental applications of poly(amic acid)-based nanomaterials. *J Environ Monit* 2011; 13: 1236–1245.
22. Javed R, Zia M, Naz S, et al. Role of capping agents in the application of nanoparticles in biomedicine and environmental remediation: recent trends and future prospects. *J Nanobiotechnol* 2020; 18: 172.
23. Sher N, Alkhalifah DHM, Ahmed M, et al. Comparative study of antimicrobial activity of silver, gold, and silver/gold bimetallic nanoparticles synthesized by green approach. *Molecules* 2022; 27(22): 7571.
24. Arora N, Thangavelu K and Karanikolos GN. Bimetallic nanoparticles for antimicrobial applications. *Front Chem* 2020; 8: 412.
25. Singh C, Mehata AK, Priya V, et al. Bimetallic Au–Ag nanoparticles: advanced nanotechnology for tackling antimicrobial resistance. *Molecules* 2022; 27(20): 6571.
26. Kalakonda P, Mandal P, Mynepally SL, et al. Comparison of multi-metallic nanoparticles—alternative antibacterial agent: understanding the role of their antibacterial properties. *J Inorg Organomet Polym Mater* 2024; 34: 2203–2218.
27. Franzolin MR, Courrol DD, Silva FR, et al. Antimicrobial activity of silver and gold nanoparticles prepared by photoreduction process with leaves and fruit extracts of *Plinia cauliflora* and *Punica granatum*. *Molecules* 2022; 27(20): 6817.
28. Sanità G, Carrese B and Lamberti A. Nanoparticle surface functionalization: how to improve biocompatibility and cellular internalization. *Front Mol Biosci* 2020; 7: 381.

29. Botteon CEA, Silva LB, Ccana-Ccapatinta GV, et al. Biosynthesis and characterization of gold nanoparticles using Brazilian red propolis and evaluation of its antimicrobial and anticancer activities. *Sci Rep* 2021; 11: 1974.
30. Prihapsara F, Artanti AN and Ni'mah LFU. Characterization and antimicrobial activity of gold nanoparticles fruit infusion of Medinilla speciosa. *J Phys Conf Ser* 2022; 2190: 012030.
31. Franci G, Falanga A, Galdiero S, et al. Silver nanoparticles as potential antibacterial agents. *Molecules* 2015; 20(5): 8856–8874.
32. Mota WS, Severino P, Kadian V, et al. Nanometrology: particle sizing and influence on the toxicological profile. *Front Nanotechnol* 2025; 7: 153.
33. Tayebi SS, Dowdall N, Hoare T, et al. Data-driven optimization of nanoparticle size using the prediction reliability enhancing parameter (PREP). *Nanoscale* 2025; 17: 19767–19784.